Cancer-associated CD43 glycoforms as target of immunotherapy

Franca Maria Tuccillo[1,*], **Camillo Palmieri**[2,*], **Giuseppe Fiume**[2], **Annamaria de Laurentiis**[2], **Marco Schiavone**[2], **Cristina Falcone**[2], **Enrico Iaccino**[2], **Ricciarda Galandrini**[3], **Cristina Capuano**[3], **Angela Santoni**[4], **Francesco Paolo D'Armiento**[5], **Claudio Arra**[6], **Antonio Barbieri**[6], **Fabrizio Dal Piaz**[7], **David Venzon**[8], **Patrizia Bonelli**[1], **Franco Maria Buonaguro**[1], **Iris Scala**[9], **Massimo Mallardo**[10], **Ileana Quinto**[2], and **Giuseppe Scala**[2]

[1]Laboratory of Molecular Biology and Viral Oncogenesis, Istituto Nazionale per lo Studio e la Cura dei Tumori "Fondazione G. Pascale"- IRCCS, Naples, Italy

[2]Department of Experimental and Clinical Medicine, University "Magna Graecia" of Catanzaro, Catanzaro, Italy

[3]Departments of Experimental Medicine, Sapienza University, Rome, Italy

[4]Department of Molecular Medicine- Istituto Pasteur - Fondazione Cenci-Bolognetti, Sapienza University, Rome, Italy

[5]Department of Advanced Biomedical Sciences, University of Naples "Federico II", Naples, Italy

[6]Animal Facility, Istituto Nazionale per lo Studio e la Cura dei Tumori "Fondazione G. Pascale"- IRCCS, Naples, Italy

[7]Department of Pharmacy, University of Salerno, Fisciano, Salerno, Italy

[8]Biostatistics and Data Management Section, National Cancer Institute, Bethesda, MD, USA

[9]Department of Pediatrics, University of Naples "Federico II", Naples, Italy

[10]Department of Molecular Medicine and Medical Biotechnology, University of Naples "Federico II", Naples, Italy

Abstract

CD43 is a sialoglycosylated membrane protein that is involved in cell proliferation and differentiation. CD43 glycoforms that are recognized by the UN1 monoclonal antibody (mAb) were expressed in lymphoblastoid T-cell lines and solid tumors, such as breast, colon, gastric, and squamous cell lung carcinomas, while unexpressed in the normal counterparts. The cancer–association of UN1/CD43 epitope suggested the possibility to use the UN1 mAb for tumor diagnosis and therapy.

In this study, we show that the UN1 mAb was endowed with anti-tumor activity *in vivo* since its passive transfer inhibited the growth of UN1-positive HPB-ALL lymphoblastoid T-cells in mice. Further, we demonstrate that tumor inhibition was due to UN1 mAb-dependent NK-mediated cytotoxicity. By screening a phage displayed random peptide library we identified the phagotope 2/165 as a mimotope of the UN1 antigen, as it harboured a peptide sequence that was specifically

Corresponding Authors: Franca Maria Tuccillo, Laboratory of Molecular Biology and Viral Oncogenesis, Istituto Nazionale per lo Studio e la Cura dei Tumori "Fondazione G. Pascale", IRCCS, via Mariano Semmola, 80131, Naples, Italy. Phone: 39-081-5903270; Fax: 39-081-5903803; f.tuccillo@istitutotumori.na.it; Ileana Quinto, Department of Experimental and Clinical Medicine, University "Magna Graecia" of Catanzaro, Viale Europa-Germaneto, 88100, Catanzaro, Italy. Phone: 39-0961-3694058; Fax: 39-0961-3694090; quinto@unicz.it.
*These authors equally contributed to this study

recognized by the UN1 mAb and inhibited the binding of the UN1 mAb to UN1-positive tumour cells. Based on sequence homology with the extracellular region of CD43 (amino acids 64 to 83), the 2/165 peptide sequence was likely mimicking the protein core of the UN1/CD43 epitope. When used as vaccine in mice, the 2/165 phagotope raised antibodies against the UN1/CD43 antigen, indicating that the 2/165 phagotope mimicked the UN1 antigen structure, and could represent a novel immunogen for cancer immunotherapy. These findings support the feasibility to use monoclonal antibodies to identify cancer-associated mimotopes for immunotherapy.

Keywords

Antibody immunotherapy; Immune response to cancer; Tumor antigens; CD43; UN1 monoclonal antibody; Mimotopes; Cancer vaccine

Introduction

CD43 is a highly sialylated and *O*-glycosylated membrane protein with the apparent molecular weight of 100–120 kDa, and is mostly expressed in hematopoietic cells, including stem cells (1). CD43 is involved in multiple functions, such as cell adhesion, apoptosis and migration (2). The UN1 monoclonal antibody (mAb) was initially selected for a high reactivity against human immature thymocytes (CD3^{dim}) (3), and recognized a CD43 epitope that included the monosaccharide GalNAc-*O*-linked to the polypeptide chain, named UN1/CD43 antigen (4). The UN1/CD43 antigen was expressed in human thymocytes, a subpopulation of peripheral blood CD4$^+$ T-lymphocytes, and some leukemic T-cell lines, such as HPB-ALL, H9, and MOLT-4 (3, 5). Moreover, the UN1/CD43 antigen was expressed at early stages of development in foetal tissues, including thymus, spleen, adrenal cortex, bronchial epithelium, and skin, and is down-regulated in ontogeny (6). The involvement of UN1/CD43 glycoforms in oncogenesis was suggested by several findings. In fact, UN1/CD43 was detected in a variety of solid tumours, including breast, colon, gastric, and squamous cell lung carcinomas, while it was undetected in the relative normal tissues and benign lesions (6, 7). In particular, the expression level of UN1/CD43 glycoforms in breast cancer cells correlated with the progression stage of the disease (7). The evidence that the UN1-type CD43 membrane proteins were expressed in cancer tissues made the UN1 mAb an attractive tool for tumor detection and immunotherapy.

Several mAbs directed against surface antigens of tumor cells are currently used for cancer therapy (8). However, mAb-based therapy has many disadvantages, such as the relatively short-lived response, the development of therapy-resistance and immune reaction overtime, and a high cost-of-production (9, 10). As alternative to the direct use of therapeutic mAb, vaccine strategies using peptide mimics of specific epitopes to elicit a humoral and cellular immune response against tumor cells could be a more effective and economical approach (11). In this regard, phage-displayed random peptide libraries (RPLs) have been used to select peptides that mimic natural epitopes, so called mimotopes, even in the absence of knowledge on the antigen structure (12). Mimotopes have been used as immunogens for raising antibodies against the natural epitope, thus representing a suitable tool for immunotherapy (13-16). In particular, the mimotope-based immunization can overcome the major limitations of glycosylated antigens, including the poor immunogenicity, the inability to stimulate a long-lasting immune response, and the difficulty to synthesize and purify large quantities of glycosylated proteins for immunization (17). To date, a few mimotopes of tumor antigens have been identified (18-21) some of which raised epitope-specific antibodies for cancer vaccine (14, 22-26).

In this study, we show that the passive transfer of the UN1 mAb inhibited the growth of UN1-positive lymphoblastoid T-cells upon xenograft in mice, being this inhibition mediated by antibody-dependent cell-mediated cytotoxicity. By screening a phage displayed RPL, we identified the phagotope 2/165 that expressed the peptide sequence mimicking the UN1/CD43 epitope, and we demonstrated that mice immunization with this phagotope elicited antibodies that specifically recognized UN1-positive cancer tissues. These findings support the possibility to target cancer-associated CD43 glycoforms by using immunotherapeutic strategies based on UN1 mAb and UN1 mimotopes.

Materials and Methods

Cells

Human thymic acute lymphocytic leukaemia HPB-ALL cells were obtained by the German Collection of Microorganisms and Cell Cultures (Braunschweig, Germany) in 2003. The cell line was expanded and cryopreserved in liquid nitrogen in the investigators laboratory, and lastly verified in 2013 using the following tests: morphology was evaluated by microscopic examination, growth curve analysis was conducted, and immunophenotype of cells was confirmed by flow cytometric analysis of cell surface markers expression. Cells were maintained (max 25 passages) in RPMI-1640 medium supplemented with with 1% L-glutamine and 10% Foetal Calf Serum (Life Technologies, Carlsbad, CA, USA).

Peripheral blood mononuclear cells were isolated from healthy donors by Ficoll-Paque gradient centrifugation (GE Healthcare Life Sciences, Piscataway, NJ, USA), as previously described (27-29). Primary cultured NK cell populations were obtained from 10-day co-cultures of PBMCs with irradiated Epstein-Barr virus-positive RPMI 8866 lymphoblastoid cell line, as previously described (30). HPB-ALL cells and primary cultured NK cells were maintained in RPMI 1640 supplemented with 1% L-glutamine and 10% Foetal Calf Serum (Life Technologies, Carlsbad, CA, USA) (31, 32).

RPL, antibodies and peptides

The f88-4/Cys5 phage displayed peptide library (GenBank Accession AF246454) was kindly provided by Dr. George P. Smith (University of Missouri, Columbia, USA). This library contains random 15-mer peptides constrained at the N-terminus of the pVIII phage coat protein with a complexity of 5.9×10^8 primary clones (33).

The IgG_1 isotype UN1 mAb was produced and purified by MAbTrap kit (GE Healthcare), as previously described (3). Antibodies used as positive controls in ADCC were as follows: OKT3 mAb (eBiosciences, San Diego, CA, USA), which recognizes a CD3 epitope that is strongly expressed on HPB-ALL cells; W6/32 mAb (eBiosciences), which recognizes a non-polymorphic epitope commonly expressed in major histocompatibility complex (MHC) class I, HLA-A, B and C, on all human nucleated cells. FITC-conjugated $F(ab')_2$ fragment of rabbit anti-mouse immunoglobulins and IgG control were purchased from Dako (Milano, Italy). Peptides were purchased from Caslo Laboratory ApS (Lyngby, Denmark).

Cell proliferation, viability, cell-cycle and apoptosis analysis

Cell proliferation was monitored by enumerating viable cells using a hemocytometer. Viability was determined by using Trypan blue dye exclusion. Cell cycle and apoptosis analysis were performed as previously described (34-36).

In vivo tumour growth analysis

Six weeks old female NU/NU nude mice (BALB/c congenic Crl:NU-Foxn1[nu] , Charles River Laboratories, Wilmington, MA, USA) were engrafted with HPB-ALL cells (5×10^6)

by subcutaneous injection into the lateral flank. Then mice were randomly assigned to two treatment groups of 5 mice: one group was treated with control mouse IgG_1 (Sigma-Aldrich, Milano, Italy), the second group was treated with the UN1 mAb. The UN1 mAb or IgG_1 control (400 µg in PBS/mouse) were injected in the tail vein of mice the day after tumor cells engraftment and the inoculation was repeated at day 7 from xenograft. The tumour size was measured by calliper, three times per week, and the tumour volume was calculated by the modified ellipsoid formula $\pi/6 \times A \times B^2$, where A is the longest and B the shortest perpendicular axis of an assumed ellipsoid. Mice were killed when the tumor volume reached a size of 4 cm^3, according to the ethical guidelines.

Complement-dependent cytotoxicity (CDC)

For assessment of cytotoxicity, triplicate HPB-ALL samples (5×10^3 cells/well) were seeded in Terasaki plates in RPMI 1640 and incubated with or without the UN1 mAb (200 µg/ml), or W6/32 mAb (100 µg/ml), or IgG_1 (100 and 200 µg/ml), in the presence or absence of the complement for 30 min at 4°C. Then, cells were treated with rabbit complement for an additional hour at 37°C. Cells were analysed by fluorescence microscopy to detect acridine orange-positive viable cells (green fluorescence) and ethidium bromide-positive dead cells (red fluorescence). Results were expressed as percentage of non-viable cells.

Antibody-dependent cellular cytotoxicity assay

NK-mediated antibody-dependent cellular cytotoxicity (ADCC) was determined using UN1-positive HPB-ALL cells. Target cells were labelled with ^{51}Cr (100 µCi/1×10^6 cells) for 1 hour at 37°C, washed twice and then incubated at room temperature for 20 minutes with the following IgG_1 isotype mAbs: UN1 mAb (0.25µg/$1x10^6$), anti-MHC class I (W6/32) (2.5µg/1×10^6), and anti-CD3 (OKT3) (0.25µg/1×10^6). Serial dilutions of effector cells, and ^{51}Cr-labelled target cells (5000 /well) were plated in triplicates in round-bottomed 96-well plates to a final volume of 200 µl RPMI supplemented with 10% FCS and 10 mM Hepes. After 4 hours incubation at 37°C, supernatant samples (30 µl) were collected from each well and counted by a β-counter instrument (TopCount, PerkinElmer Life and Analytical Sciences, Monza, Italy). Spontaneous release of ^{51}Cr was evaluated by incubating the target cells with medium alone, whereas total release was evaluated by incubating target cells with SDS 10%. Percent specific ^{51}Cr release was calculated according to the following formula: percent specific release = (experimental release-spontaneous release) /(maximum release-spontaneous release) $\times$ 100. Lytic units (LU) represent the number of effector cells required to mediate 20% lysis of target cells and were calculated by using the descending phase of curves generated by ^{51}Cr release assay over the range of effector/target cell ratios, as previously reported (37).

Immunological screening of phage displayed RPLs

Specific phage clones for the UN1 mAb were isolated from the library by two rounds of affinity selection, as previously described (38, 39). To this end, the UN1 mAb (10 µg) was linked to streptavidin-conjugated magnetic beads (Promega, Madison, WI, USA), which had been coated with 10 µg of goat anti-mouse IgG (Fc-specific) biotin-conjugated Ab (Sigma-Aldrich) in 200 µl of beads suspension. A total of 3×10^{10} transducing units (TU) of phages from the library were added and incubated for 16 hours at 4°C. After extensive washing, bound phages were eluted with 0.1 M HCl/glycine buffer pH 2.2, 1 mg/ml BSA, and neutralized with 1 M Tris pH 9.1. Eluted phages were amplified by infection of K91BK bacteria, and purified from plaques for a second round of affinity selection. Phage colonies were transferred according to an ordered grid on a lawn of K91BK cells on LB agar plates supplemented with 1mM IPTG. Nitrocellulose filters were layered onto these plates and incubated overnight at 37°C. Filters were blocked for 2 hours with blocking buffer ($1\times$ PBS, 5% non-fat dry milk, 0.1% NP40, 0.01% NaN_3) at room temperature and incubated O/N at

4°C with the UN1 mAb (1 μg/ml) in blocking buffer. Then, filters were washed with washing buffer (1× PBS, 0.1% NP40) and incubated with alkaline phosphatase-conjugated anti-mouse IgG (Fc specific) secondary antibody (Sigma-Aldrich) at the dilution of 1:5000 for 4 hours at 4°C. After extensive washing, filters were incubated in developing solution (1-Step NBT/BCIP, Pierce, Thermo Scientific, Rockford, IL, USA). Collected phage supernatants from positive clones were further analysed by ELISA.

ELISA

For assaying phage reactivity to antibodies or sera, multiwell plates (Immunoplates Maxisorp, Nunc, Milano, Italy) were coated with 10 μg/ml anti-fd bacteriophage Abs (Sigma-Aldrich) in 50 mM $NaHCO_3$, pH 9.6 overnight at 4°C. After blocking with Blocking Buffer (BB) (1× PBS, 5% non-fat dry milk, 0.05% Tween 20, 0.05% NaN_3) for 1 hour at 37°C, the BB was discarded, and a mixture of 50 μL of BB and 50 μL of phage supernatant was added to each well. After incubation for 1 hour at 37°C, plates were washed six times with Washing Buffer (WB) (1× PBS, 0.05% Tween 20, 0.05% NaN_3). Then, UN1 mAb (5 μg/mL) or sera at the indicated dilution were resuspended in BB and added to the wells. After an O/N incubation at 4°C, plates were washed 6× with WB, and a 1:5000 dilution in BB of a goat anti-mouse IgG (Fc specific) alkaline phosphatase antibody (Sigma-Aldrich) was added to wells. Alkaline phosphatase was revealed by incubation with p-nitrophenyl phosphate (1 mg/ml) in 1× diethanolamine substrate buffer (Pierce Thermo Scientific). Optical density (OD) at 450 nm (OD_{405}) and 620 nm (OD_{620}) were measured by an ELISA reader (Tecan, Männedorf, Switzerland), and values were expressed as difference between OD_{405} and OD_{620}. Wild type phage was used as negative control (40).

For assaying peptide reactivity to antibodies or sera, multiwell plates were coated with the indicated peptide (5 μg/mL) in 1× PBS pH 7.4. After blocking with BB, the UN1 mAb (5 μg/ml), or the indicated mice sera were diluted in blocking buffer and incubated O/N at 4°C. The following steps were as described above. A scrambled peptide was used as a negative control.

Surface Plasmon Resonance

Surface plasmon resonance (SPR) was performed using Biacore 3000 optical biosensor equipped with research-grade CM5 sensor chips (Biacore GE Healthcare), as previously described (41). Experimental details are provided in Supplementary Materials and Methods.

Competition assay of UN1 mAb binding

The UN1 mAb (0.37 μg/mL) was pre-incubated O/N at 4°C with CsCl-purified phages (3×10^{12} up to 3×10^8 phage particles/ml), or with synthetic peptides (0.04 μg/mL up to 400 μg/mL). The mixture was added to HPB-ALL cells (5×10^5) and incubated for 30 min at 4°C. After washing, the cells were incubated for additional 30 min at 4°C with FITC-conjugated rabbit anti-mouse immunoglobulins F(ab')2, and analyzed with BD FACSCalibur cytometer. Results were analyzed by CellQuest software (BD Biosciences, Erembodegem, Belgium) (42).

Mice immunization

Five-six week old female Balb/c mice (Harlan, Udine, Italy) were immunized by intra-peritoneal injection of CsCl-purified 2/165 phage particles, or wild type phage at weeks 0, 3, 6, 9, 12, 15, 18. The animals were bled at day 0 and 7-10 days after the 2nd, 4th and 6th boost. Phages were injected as PBS suspension in CFA (Freund's complete adjuvant) at week 0 or IFA (Freund's incomplete adjuvant) at a concentration of 6×10^{12} phage particles/

mL. Serum IgGs from mice immunized with 2/165 phage, or wild type phage, or not-immunized were purified by MAbTrap kit (GE Healthcare).

In vivo toxicity

Serum levels of inflammatory interleukin-1-β (IL1-β) were measured by ELISA (e-Biosciences), according to the manufacturer's instructions. The hepatotoxicity marker glutathione (GSH) and lactate dehydrogenase (LDH) were assayed by a colorimetric assay (Promega), according to the manufacturer's instructions.

Immunoaffinity purification of antibodies

Immunoglobulins were purified by incubating mice sera at 1:10 dilution in multi-well plates coated with 5×10^{12}/ml CsCl-purified phages. After extensive washing, the bound immunoglobulins were eluted with 0.1 M glycine-HCl buffer pH 2.7, 10 µg/ml BSA immediately neutralized with 2 M Tris-HCl pH 9.4, and concentrated using Microcon Ultracel YM-30 (Millipore, Bedford, MA, USA).

Immunohistochemistry

Surgical specimens were derived from breast and gastric cancer tissues of the patients hospitalized at the clinical surgery Federico II University of Naples. The informed consent to research activity was expressed by patients at the time of surgery for excision of neoplasia, analysed at the section of Pathological Anatomy (department of advanced biomedical sciences Federico II University of Naples). Immunohistochemical analysis was performed as previously described (6, 7). Experimental details are provided in Supplementary Materials and Methods.

Statistical analysis

Statistical analysis of tumor growth (Wilcoxon rank sum test and Wei-Johnson test) and survival (Long-Rank Mantel-Cox test) were performed with GraphPad Prism 5 program (GraphPad Software Inc., San Diego, CA). For ADCC assay, statistical analysis was performed using Prism software (GraphPad Software Inc.). Data were analysed using paired two-tailed Student's t test. Differences were considered as statistically significant at the 95% level ($p < 0.05$).

Ethics Statement

This study was carried out according to the recommendations of the Institutional animal care guidelines, Italian D.L. n. 116 of 27 January 1992 and European Communities Council Directive 2010/63EU.

Results

UN1 mAb inhibited the tumor growth of UN1-positive leukemic T-cells in nude mice

Based on the evidence that the UN1 mAb specifically bound to UN1/CD43-positive neoplastic cells (6, 7), we addressed the question of whether it could interfere the tumor growth *in vivo*. To this end, ten female six-weeks old NU/NU nude mice were tumor engrafted by subcutaneous injection of UN1-positive HPB-ALL cells into the lateral flank. Then, mice were randomly divided in two groups (5 animals/group) and treated with the UN1 mAb or IgG$_1$ control (400 µg/mouse) by injection in the tail vein at day 1 and 7 after tumor engraftment. Tumor onset and volume were monitored from day 0 up to 31, when all mice of the IgG$_1$ control group died. Tumor onset was observed at day 17 in IgG$_1$-treated mice, while it was delayed up to day 24 in UN1 mAb-treated mice. A statistically significant inhibition of tumor growth was observed in UN1 mAb-treated mice as compared to IgG$_1$-

treated controls from day 17 to 31 ($p < 0.032$ by the Wilcoxon rank sum test and $p = 0.024$ by Wei-Johnson test) (Figure 1A). Mice survival was also significantly affected by the UN1 mAb treatment. In fact, the animal group treated with UN1 mAb showed 40% survival rates at day 50 as compared to the death of IgG$_1$-treated control group ($p = 0.0031$ by log-rank Mantel-Cox test) (Figure 1B). These data showed that mAb UN1 treatment had an anti-tumour activity in the HPB-ALL tumor xenograft mice model.

UN1 mAb caused HPB-ALL cell lysis *via* antibody-dependent cell-mediated cytotoxicity

To understand the mechanism of UN1 mAb-inhibition of HPB-ALL tumor growth, we analysed the direct effect of the UN1 mAb on cell growth by incubating the HPB-ALL cells with the UN1 mAb (1 up to 25 µg/ml), or IgG$_1$ negative control. The UN1 mAb did not affect the proliferation rate, cell cycle, the number of viable and apoptotic cells as compared to untreated or IgG-treated cells (Fig. S1 A-D). Further, we analysed whether the UN1 mAb could act *via* complement-mediated cell lysis. Cytotoxicity was assessed by incubating HPB-ALL cells with or without UN1 mAb, in presence or absence of the complement. W6/32 mAb and IgG were included as positive and negative controls, respectively. Differently from W6/32 mAb, the UN1 mAb did not affect cell lysis (Fig 1C).

The antibody-dependent cell-mediated cytotoxicity (ADCC) is triggered by the binding of antibody-opsonised tumour cells to FcγRIIIA/CD16 of NK cells resulting in tumour cell lysis. Thus, we reasoned that ADCC could be a mechanism of UN1 mAb-dependent tumor inhibition. To evaluate whether the UN1 mAb induced CD16-mediated ADCC, HPB-ALL cells were opsonized with the UN1 mAb, or OKT3 or W6/32 mAbs as positive controls. Cultured primary NK cells from nine healthy donors were tested in a standard ADCC assay. A significant antibody-mediated lysis of tumor cells ($p = 0.0026$) was observed in the UN1 mAb-opsonized samples as compared to not-opsonised controls, being the UN1-opsonized targets were killed more efficiently in seven out of nine donors (Fig. 1D). Moreover, ADCC induced by UN1 mAb was slightly lower as compared to W6/32 mAb (mean 21.9% *vs* 24.4%), or OKT3 mAb (mean 21.9% *vs* 32.3%) (Fig. 1D). The ability of UN1 mAb to induce ADCC was also supported by the analysis of lytic units within the same donor, which were calculated for the whole curve effector/target cells (E/T) ratio (Fig. 1E). For the UN1, OKT3 and W6/32 mAbs the strenght of binding to HBP-ALL cells directly correlated with their ADCC potency (Fig. S2A), which was likely due to the expression levels of cognate antigens on cell surface.

Identification of the UN1 mimotope by phage displayed RPL

Based on the UN1 mAb inhibition of UN1-positive tumor cells, we reasoned that the identification of the UN1/CD43 epitope recognized by the UN1 mAb could be useful for developing novel immunogens for cancer immunotherapy. To this end, we used the UN1 mAb to screen an f88-4/Cys5 phage displayed peptide library by two rounds of affinity selection. A phage enrichment was observed during the selection as the output/input phage ratio increased from 1.1×10^{-6} after round I to 1.2×10^{-2} after round II. After an immunoscreening step, 174 single phage clones were recovered and tested by ELISA for specific binding to the UN1 mAb and, among them, 153 clones were found to react with the UN1 mAb. OD values of positive phagotopes ranged between 4 - 40 folds higher than wild type phage (Fig. 2A). Based on these results, 28 phage clones showing the strongest positive signal were selected for DNA sequencing, which yielded 11 different peptide mimotopes sequences (Table 1). MUSCLE-based alignment analysis (http://www.ebi.ac.uk/Tools/msa/muscle/) showed a significant homology between the 11 peptides and the human protein CD43 (Fig. 2B), which is the natural antigen recognized by UN1 mAb (4). Indeed, the homology region of the 11 amino acidic sequences of mimotopes falls in the extra-cellular domain of CD43 (amino acids 64 to 83), a region that undergoes highly *O*-linked

glycosylation (4). Among the 11-selected clones, the phagotope 2/165 was chosen due to the strongest reactivity against UN1 mAb in ELISA (Table 1).

Two peptides were synthesized corresponding to the insert of the 2/165 phagotope (W15 peptide: TPHTCKLLDECVPLW) and a longer synthetic peptide containing the W15 peptide sequence with additional amino acid residues flanking the insert of the phagotope 2/165 (G23 peptide: SFAATPHTCKLLDECVPLWPAEG). As negative control, a scrambled peptide was synthesized (TCLAPDVPEPLSHCWAGETFKLA). By surface plasmon resonance (SPR), we measured binding affinity of the peptides W15 and G23 to the UN1 mAb. Sensorgrams showed that G23 and W15 peptides exhibited similar affinities for the UN1 mAb (K_D 155 nM and 142 nM, respectively) while the scrambled peptide failed to give the SPR signal (Fig. 2C).

Phagotope 2/165 and UN1 peptide mimotopes competed the binding of UN1 mAb to tumor cells

Next, we determined whether the phage clone 2/165 and the peptides W15 and G23 mimic the structure of the UN1 epitope. To this end, we performed a competitive inhibition assay for the binding of the UN1 mAb to the HPB-ALL cells in presence or absence of the phagotope 2/165 or the peptide mimotopes. The binding of UN1 mAb to HPB-ALL cells was significantly reduced in presence of phage 2/165 (Fig. 3A, B), G23 or W15 peptides (Fig. 3C, D) in a dose-related manner. This effect was not observed in presence of wild type phage or scrambled peptide (Fig. 3A-D). Conversely, the phage 2/165 and the peptides G23 and W15 did not compete the binding of W6/32 mAb, an anti-human HLA class I antigen (Fig. S2B). As additional evidence of structural similarity to the UN1/CD43 epitope, the phage 2/165 and G23 competed the binding of UN1 mAb to UN1-positive breast and gastric cancer tissues, while the wild type phage and scrambled peptide did not (Fig. S3). These results indicated that the phagotope 2/165 as well as the derived G23 and W15 peptides mimicked the conformation of the UN1/CD43 epitope.

Mice immunization with phagotope 2/165 elicited antibodies against the UN1/CD43 natural antigen

Filamentous phage can be used as immunogen as they elicit a strong antibody response in different animal systems (43, 44). Thus, we analysed the immunogenicity of the phagotope 2/165 in mice. Balb/c mice (5 animals/group) were immunized with the phage 2/165, or wild type phage, and the collected sera were analysed for reactivity against the wild type phage, G23 or a scrambled peptide as control (Fig. 4). Both wild type phage- and 2/165 phagotope-immunized mice appeared healthy and did not show any ill-effect. Moreover, both groups of immunized mice showed levels of serum inflammatory cytokine IL1-β and hepatotoxicity marker GSH and LDH in the range of normality (Table 2), indicating that phage immunization was not toxic.

As expected, both groups of immunized mice developed a strong and comparable antibody response against the wild type phage, while control serum from a non-immunized mouse showed no reactivity (Fig. 4A, B, left panels). However, the phagotope 2/165-immunized mice sera showed a specific immune response against the UN1 mimotope G23 peptide (1:20,000 up to 1:100,000 antibody titer) (Fig. 4A, middle panel), while they were unreactive against the scrambled peptide (Fig. 4A, right panel). As negative control, the pre-immune and wild type-phage immunized mice sera did not show any detectable reactivity against the G23 (Fig. 4B, middle panel), or scrambled peptide (Fig. 4B, right panel). As further analysis of 2/165 phagotope-induced antibodies recognition of UN1 epitope, immunoglobulins were affinity-purified from sera of 2/165 phagotope immunized mice or pre-immune sera using the 2/165 phagotope or wild type phage as ligand. The

immunoglobulins (Igs) eluted from 2/165 phagotope (2/165 Igs) reacted with the G23 peptide, whereas Igs eluted from wild type phage (wt Igs) did not (Fig. S4A). Further, by flow cytometry we confirmed that the 2/165 Igs bound to the HPB-ALL cells (Fig. S4B). On the basis of the reported reactivity of the UN1 mAb with tumor tissues (6, 7), we tested whether the 2/165 IgGs detected UN1-positive human breast and gastric cancer by immunohistochemistry. We found that 2/165 IgGs specifically reacted with breast and gastric cancer tissues with a pattern similar to the one observed with the UN1 mAb (Fig. 5). Conversely, no reactivity against the cancer tissues was observed using the wt IgGs or pre-immune IgGs (Fig. 5). The binding specificity of the 2/165 IgGs to UN1-positive cancer tissues was confirmed by competition assays. Indeed, the pre-incubation of 2/165 IgGs with the 2/165 phagotope or the UN1 mimotope G23 peptide inhibited the binding of 2/165 IgGs to UN1-positive tumor tissues, confirming the binding specificity of 2/165 IgGs to the UN1 epitope exposed on tumor cells (Fig. 6).

Discussion

CD43 is a transmembrane sialoglycoprotein that is mostly expressed in haematopoietic cells, and tumor cells of non-haematopoietic origin. CD43 signalling activates cellular pathways leading to activation of NF-κB and AP1 transcription factors that up-regulate the expression of pro-survival and proliferation genes (45). Deregulation of CD43 signalling can promote cancer phenotype (45). We previously reported that specific CD43 glycoforms were recognized by the UN1 mAb and were highly expressed in lymphoblastoid T-cell lines and several solid tumors (4, 6, 7). In particular, the expression of UN1-type CD43 in breast cancer correlated with the grade of malignancy, suggesting that the specific CD43 glycoforms could promote an altered proliferation signalling and cause cancer progression (6, 7). Based on this evidence, the UN1 mAb was considered a suitable tool for cancer immunophenotyping.

The aim of this study was to evaluate the immunotherapeutic activity of the UN1 mAb based on the ability of this monoclonal antibody to target specifically the cancer cells expressing the UN1-type CD43 glycoforms. We observed that the passive transfer of the UN1 mAb inhibited the growth of UN1-positive HPB-ALL lymphoblastoid T-cells upon xenograft in mice, suggesting a possible use of this antibody for cancer immunotherapy. We excluded that tumor growth inhibition was due to direct cytostatic or cytotoxic activity of the UN1 mAb since the proliferation rate, cell cycle, and viability of HPB-ALL cells were unaffected by the UN1 mAb in cell culture. Conversely, the UN1 mAb induced the *in vitro* lysis of HPB-ALL cells *via* antibody-dependent NK-mediated cytotoxicity. Based on these findings, the UN1 mAb behaved similarly to the antibodies that are currently used in cancer therapy against specifically or differentially expressed tumor antigens, such as anti-CD20 (rituximab), anti Her-2/neu (trastuzumab), and anti-EGFR (cetuximab) (46). It is worth mentioning that such validated anti-cancer therapeutic mAbs exhibited multiple effector mechanisms for their *in vivo* anti-tumour activity (46). Even though additional mechanisms of UN1 mAb action require further investigation, such as receptor down-modulation, ligand blockade or antibody-dependent cellular phagocytosis (ADCP), the *in vitro* analysis performed in this study indicates that ADCC could be a major mechanism of *in vivo* anti-tumor activity.

We also explored the possibility to generate a mimotope of the UN1/CD43 epitope to be used as immunogen for eliciting highly specific Abs against the UN1-positive tumor tissues. By screening an f88-4/Cys5 phage displayed peptide library with the UN1 mAb, we identified and characterized eleven peptide binders of the UN1 mAb. Among the selected phage clones, the peptide insert of phagotope 2/165 was a true UN1/CD43 epitope mimic because it was specifically recognized by the UN1 mAb and inhibited the binding of the

UN1 mAb to the UN1/CD43 natural antigen, meeting the previously established guidelines for specificity and mimicry testing (47). Several studies have indicated that cysteine-constrained phage displayed peptides are endowed with a stabilized conformation that allows the isolation of cyclic peptides with a higher affinity toward a bait as compared to non-constrained, linear peptides (48). Moreover, cysteine-constrained phage-derived peptides have been shown to bind the cognate ligand outside of the phage coat protein (38), either in a different protein back-bone (49), or when coupled to therapeutic agents (50). In these settings, the 2/165 peptide could represent a flexible tool for the targeted therapy of UN1-positive tumor cells.

Bioinformatics-based analysis identified a significant sequence homology between the eleven UN1 peptide mimotopes and the amino acids 64 to 83 contained in the extra-cellular domain of CD43 that undergoes heavy O-glycosylation. These findings agree with our previous observation that the monosaccharide GalNAc-*O*-linked to the CD43 peptide core was an essential component of the UN1 epitope (4), and suggests the hypothesis that the UN1 peptide core overlaps the sequence from 64 to 83 amino acids of the CD43 extra-cellular domain.

For vaccine purpose, glycosylated antigens are difficult to synthesize and purify in large quantities, and usually induce a poor immune response with short-lived IgM-type antibodies. Novel strategies of vaccine production are required to overcome these major limitations (17). Phage mimotopes of cancer antigens (18, 21-23), revealed a promising activity as immunogens by eliciting a strong cross-reactive antibody response against the selected natural antigens. Here, we have demonstrated that the phagotope 2/165 mimicked the cancer-associated UN1/CD43 epitope and induced in immunized mice specific antibodies against the UN1/CD43 antigen. In fact, purified immunoglobulins from 2/165 phagotope-immunized mice sera specifically reacted with several UN1-positive cancer tissues, as confirmed by competition assays. Further, the UN1 mimotope-induced antibodies were IgG isotype, a peculiar feature of a long-standing-immune response, indicating that the mimotope-based immunization can overcome the poor immunogenicity of purified glycosylated antigens.

Based on these results, the UN1/CD43 epitope may represent a suitable target for cancer immunotherapy, and UN1 mimotopes, such as 2/165 phagotope and derivative G23 peptide here described, are promising cancer vaccine candidates for UN1-positive tumors.

Supplementary Material

Refer to Web version on PubMed Central for supplementary material.

Acknowledgments

References

1. Kadaja-Saarepuu L, Looke M, Balikova A, Maimets T. Tumor suppressor p53 down-regulates expression of human leukocyte marker CD43 in non-hematopoietic tumor cells. International journal of oncology. 2012; 40:567–76. [PubMed: 21947346]

2. Ostberg JR, Barth RK, Frelinger JG. The Roman god Janus: a paradigm for the function of CD43. Immunology today. 1998; 19:546–50. [PubMed: 9864944]

3. Tassone P, Bond H, Bonelli P, Tuccillo F, Valerio G, Petrella A, et al. UN1, a murine monoclonal antibody recognizing a novel human thymic antigen. Tissue antigens. 1994; 44:73–82. [PubMed: 7817381]

4. de Laurentiis A, Gaspari M, Palmieri C, Falcone C, Iaccino E, Fiume G, et al. Mass spectrometry-based identification of the tumor antigen UN1 as the transmembrane CD43 sialoglycoprotein. Molecular & cellular proteomics : MCP. 2011; 10:M111 007898. [PubMed: 21372249]

5. Cecco L, Bond HM, Bonelli P, Tuccillo F, Cerra M, Tassone P, et al. Purification and characterization of a human sialoglycoprotein antigen expressed in immature thymocytes and fetal tissues. Tissue antigens. 1998; 51:528–35. [PubMed: 9672151]

6. Tassone P, Tuccillo F, Bonelli P, D'Armiento FP, Bond HM, Palmieri C, et al. Fetal ontogeny and tumor expression of the early thymic antigen UN1. International journal of oncology. 2002; 20:707–11. [PubMed: 11894113]

7. Tassone P, Bonelli P, Tuccillo F, Bond HM, D'Armiento FP, Galea E, et al. Differential expression of UN1, early thymocyte-associated sialoglycoprotein, in breast normal tissue, benign disease and carcinomas. Anticancer research. 2002; 22:2333–40. [PubMed: 12174923]

8. Bhutani D, Vaishampayan UN. Monoclonal antibodies in oncology therapeutics: present and future indications. Expert opinion on biological therapy. 2013; 13:269–82. [PubMed: 23286740]

9. Hong CW, Zeng Q. Awaiting a new era of cancer immunotherapy. Cancer research. 2012; 72:3715–9. [PubMed: 22815525]

10. Hansel TT, Kropshofer H, Singer T, Mitchell JA, George AJ. The safety and side effects of monoclonal antibodies. Nature reviews Drug discovery. 2010; 9:325–38.

11. Purcell AW, McCluskey J, Rossjohn J. More than one reason to rethink the use of peptides in vaccine design. Nature reviews Drug discovery. 2007; 6:404–14.

12. Bratkovic T. Progress in phage display: evolution of the technique and its application. Cellular and molecular life sciences : CMLS. 2010; 67:749–67. [PubMed: 20196239]

13. Knittelfelder R, Riemer AB, Jensen-Jarolim E. Mimotope vaccination--from allergy to cancer. Expert opinion on biological therapy. 2009; 9:493–506. [PubMed: 19344285]

14. Sharav T, Wiesmuller KH, Walden P. Mimotope vaccines for cancer immunotherapy. Vaccine. 2007; 25:3032–7. [PubMed: 17276556]

15. Arnaiz B, Madrigal-Estebas L, Todryk S, James TC, Doherty DG, Bond U. A novel method to identify and characterise peptide mimotopes of heat shock protein 70-associated antigens. Journal of immune based therapies and vaccines. 2006; 4:2. [PubMed: 16603084]

16. James TC, Bond U. Molecular mimics of the tumour antigen MUC1. PloS one. 2012; 7:e49728. [PubMed: 23166757]

17. Kozbor D. Cancer vaccine with mimotopes of tumor-associated carbohydrate antigens. Immunologic research. 2010; 46:23–31. [PubMed: 19763891]

18. Riemer AB, Kraml G, Scheiner O, Zielinski CC, Jensen-Jarolim E. Matching of trastuzumab (Herceptin) epitope mimics onto the surface of Her-2/neu--a new method of epitope definition. Molecular immunology. 2005; 42:1121–4. [PubMed: 15829301]

19. Riemer AB, Klinger M, Wagner S, Bernhaus A, Mazzucchelli L, Pehamberger H, et al. Generation of Peptide mimics of the epitope recognized by trastuzumab on the oncogenic protein Her-2/neu. J Immunol. 2004; 173:394–401. [PubMed: 15210798]

20. Geiser M, Schultz D, Le Cardinal A, Voshol H, Garcia-Echeverria C. Identification of the human melanoma-associated chondroitin sulfate proteoglycan antigen epitope recognized by the antitumor monoclonal antibody 763.74 from a peptide phage library. Cancer research. 1999; 59:905–10. [PubMed: 10029083]

21. Shanmugam A, Suriano R, Chaudhuri D, Rajoria S, George A, Mittelman A, et al. Identification of PSA peptide mimotopes using phage display peptide library. Peptides. 2011; 32:1097–102. [PubMed: 21539876]

22. Riemer AB, Kurz H, Klinger M, Scheiner O, Zielinski CC, Jensen-Jarolim E. Vaccination with cetuximab mimotopes and biological properties of induced anti-epidermal growth factor receptor antibodies. Journal of the National Cancer Institute. 2005; 97:1663–70. [PubMed: 16288119]

23. Riemer AB, Hantusch B, Sponer B, Kraml G, Hafner C, Zielinski CC, et al. High-molecular-weight melanoma-associated antigen mimotope immunizations induce antibodies recognizing melanoma cells. Cancer immunology, immunotherapy : CII. 2005; 54:677–84.

24. Bramswig KH, Knittelfelder R, Gruber S, Untersmayr E, Riemer AB, Szalai K, et al. Immunization with mimotopes prevents growth of carcinoembryonic antigen positive tumors in BALB/c mice. Clinical cancer research : an official journal of the American Association for Cancer Research. 2007; 13:6501–8. [PubMed: 17975163]

25. Jasinska J, Wagner S, Radauer C, Sedivy R, Brodowicz T, Wiltschke C, et al. Inhibition of tumor cell growth by antibodies induced after vaccination with peptides derived from the extracellular domain of Her-2/neu. International journal of cancer Journal international du cancer. 2003; 107:976–83. [PubMed: 14601058]

26. Hartmann C, Muller N, Blaukat A, Koch J, Benhar I, Wels WS. Peptide mimotopes recognized by antibodies cetuximab and matuzumab induce a functionally equivalent anti-EGFR immune response. Oncogene. 2010; 29:4517–27. [PubMed: 20514015]

27. Palmieri C, Trimboli F, Puca A, Fiume G, Scala G, Quinto I. Inhibition of HIV-1 replication in primary human monocytes by the IkappaB-alphaS32/36A repressor of NF-kappaB. Retrovirology. 2004; 1:45. [PubMed: 15613239]

28. Fiume G, Vecchio E, De Laurentiis A, Trimboli F, Palmieri C, Pisano A, et al. Human immunodeficiency virus-1 Tat activates NF-kappaB via physical interaction with IkappaB-alpha and p65. Nucleic acids research. 2012; 40:3548–62. [PubMed: 22187158]

29. Fiume G, Rossi A, de Laurentiis A, Falcone C, Pisano A, Vecchio E, et al. Eukaryotic Initiation Factor 4H Is under Transcriptional Control of p65/NF-kappaB. PloS one. 2013; 8:e66087. [PubMed: 23776612]

30. Capuano C, Paolini R, Molfetta R, Frati L, Santoni A, Galandrini R. PIP2-dependent regulation of Munc13-4 endocytic recycling: impact on the cytolytic secretory pathway. Blood. 2012; 119:2252–62. [PubMed: 22271450]

31. Spatuzza C, Schiavone M, Di Salle E, Janda E, Sardiello M, Fiume G, et al. Physical and functional characterization of the genetic locus of IBtk, an inhibitor of Bruton's tyrosine kinase: evidence for three protein isoforms of IBtk. Nucleic acids research. 2008; 36:4402–16. [PubMed: 18596081]

32. Tallerico R, Todaro M, Di Franco S, Maccalli C, Garofalo C, Sottile R, et al. Human NK cells selective targeting of colon cancer-initiating cells: a role for natural cytotoxicity receptors and MHC class I molecules. J Immunol. 2013; 190:2381–90. [PubMed: 23345327]

33. Schiavone M, Fiume G, Caivano A, de Laurentiis A, Falcone C, Masci FF, et al. Design and Characterization of a Peptide Mimotope of the HIV-1 gp120 Bridging Sheet. International journal of molecular sciences. 2012; 13:5674–99. [PubMed: 22754323]

34. Puca A, Fiume G, Palmieri C, Trimboli F, Olimpico F, Scala G, et al. IkappaB-alpha represses the transcriptional activity of the HIV-1 Tat transactivator by promoting its nuclear export. The Journal of biological chemistry. 2007; 282:37146–57. [PubMed: 17942396]

35. Bonelli P, Tuccillo FM, Calemma R, Pezzetti F, Borrelli A, Martinelli R, et al. Changes in the gene expression profile of gastric cancer cells in response to ibuprofen: a gene pathway analysis. The pharmacogenomics journal. 2011; 11:412–28. [PubMed: 20548326]

36. Fiume G, Rossi A, Di Salle E, Spatuzza C, Mallardo M, Scala G, et al. Computational analysis and in vivo validation of a microRNA encoded by the IBTK gene, a regulator of B-lymphocytes differentiation and survival. Computational biology and chemistry. 2009; 33:434–9. [PubMed: 19782003]

37. Trinchieri G. Biology of natural killer cells. Adv Immunol. 1989; 47:187–376. [PubMed: 2683611]

38. Palmieri C, Falcone C, Iaccino E, Tuccillo FM, Gaspari M, Trimboli F, et al. In vivo targeting and growth inhibition of the A20 murine B-cell lymphoma by an idiotype-specific peptide binder. Blood. 2010; 116:226–38. [PubMed: 20363775]

39. Causa F, Della Moglie R, Iaccino E, Mimmi S, Marasco D, Scognamiglio PL, et al. Evolutionary screening and adsorption behavior of engineered M13 bacteriophage and derived dodecapeptide for selective decoration of gold interfaces. Journal of colloid and interface science. 2013; 389:220–9. [PubMed: 23031494]

40. Paduano F, Ortuso F, Campiglia P, Raso C, Iaccino E, Gaspari M, et al. Isolation and functional characterization of peptide agonists of PTPRJ, a tyrosine phosphatase receptor endowed with tumor suppressor activity. ACS chemical biology. 2012; 7:1666–76. [PubMed: 22759068]

41. Vitagliano L, Fiume G, Scognamiglio PL, Doti N, Cannavo R, Puca A, et al. Structural and functional insights into IkappaB-alpha/HIV-1 Tat interaction. Biochimie. 93:1592–600. [PubMed: 21664225]

42. Janda E, Palmieri C, Pisano A, Pontoriero M, Iaccino E, Falcone C, et al. Btk regulation in human and mouse B cells via protein kinase C phosphorylation of IBtkgamma. Blood. 2011; 117:6520–31. [PubMed: 21482705]

43. van Houten NE, Zwick MB, Menendez A, Scott JK. Filamentous phage as an immunogenic carrier to elicit focused antibody responses against a synthetic peptide. Vaccine. 2006; 24:4188–200. [PubMed: 16488517]

44. Chen X, Scala G, Quinto I, Liu W, Chun TW, Justement JS, et al. Protection of rhesus macaques against disease progression from pathogenic SHIV-89.6PD by vaccination with phage-displayed HIV-1 epitopes. Nature medicine. 2001; 7:1225–31.

45. Santana MA, Pedraza-Alva G, Olivares-Zavaleta N, Madrid-Marina V, Horejsi V, Burakoff SJ, et al. CD43-mediated signals induce DNA binding activity of AP-1, NF-AT, and NFkappa B transcription factors in human T lymphocytes. The Journal of biological chemistry. 2000; 275:31460–8. [PubMed: 10908570]

46. Weiner LM, Surana R, Wang S. Monoclonal antibodies: versatile platforms for cancer immunotherapy. Nature reviews Immunology. 2010; 10:317–27.

47. Riemer A, Scheiner O, Jensen-Jarolim E. Allergen mimotopes. Methods. 2004; 32:321–7. [PubMed: 14962767]

48. Giebel LB, Cass RT, Milligan DL, Young DC, Arze R, Johnson CR. Screening of cyclic peptide phage libraries identifies ligands that bind streptavidin with high affinities. Biochemistry. 1995; 34:15430–5. [PubMed: 7492543]

49. Curnis F, Sacchi A, Borgna L, Magni F, Gasparri A, Corti A. Enhancement of tumor necrosis factor alpha antitumor immunotherapeutic properties by targeted delivery to aminopeptidase N (CD13). Nature biotechnology. 2000; 18:1185–90.

50. Arap W, Pasqualini R, Ruoslahti E. Cancer treatment by targeted drug delivery to tumor vasculature in a mouse model. Science. 1998; 279:377–80. [PubMed: 9430587]
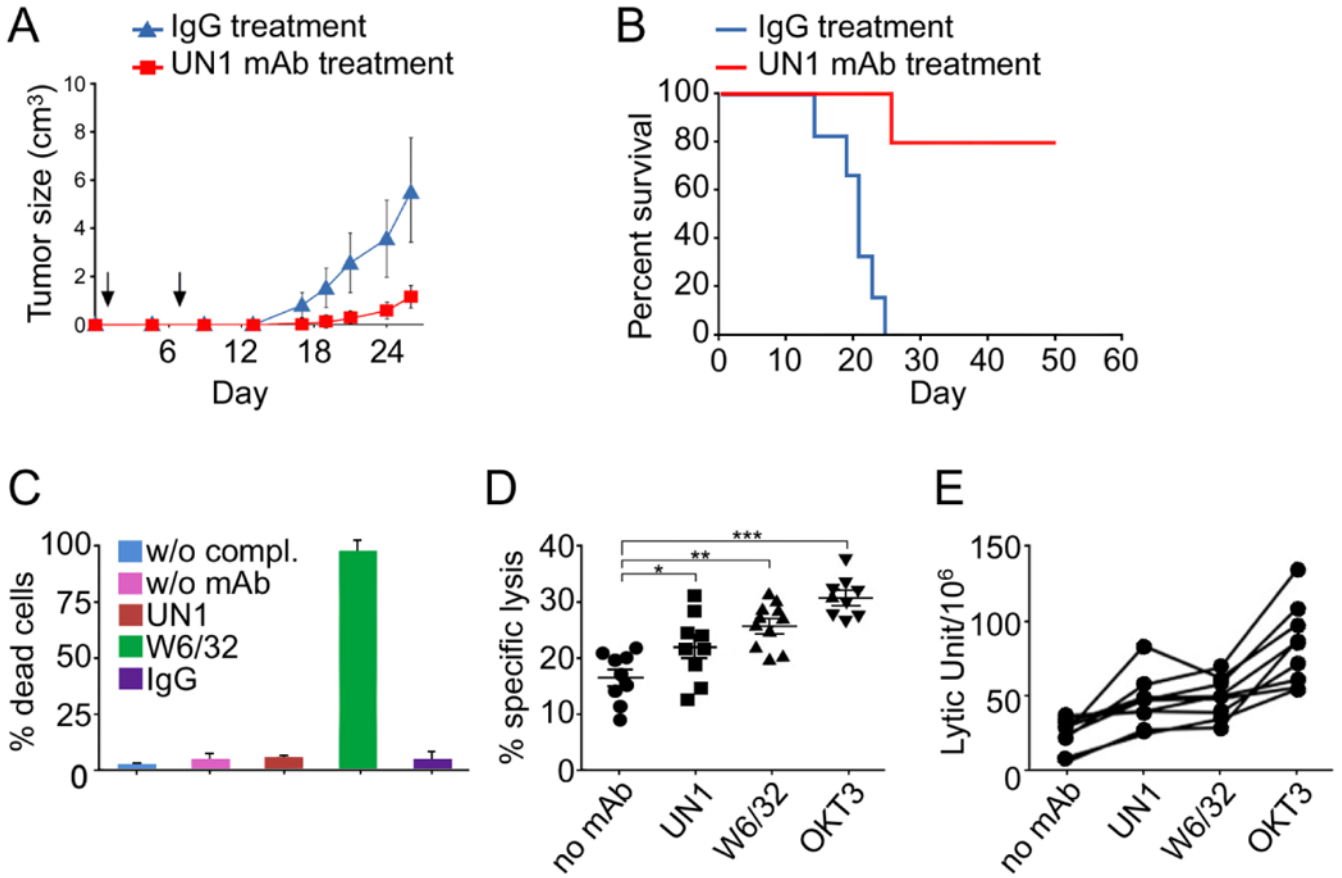
Fig. 1. UN1 mAb inhibited UN1-positive tumor growth *via* ADCC
(A) UN1 mAb treatment resulted in tumor growth inhibition in mice engrafted with HPB-ALL lymphoblastoid T-cells. Tumour growth curves (mean tumour volume ± SEM) in HPB-ALL xenograft mice models treated with control IgG (400 µg in PBS/mouse) or UN1 mAb (400 µg in PBS/mouse). Arrows indicate the time of antibodies administration. A representative of 2 independent experiments with similar results is shown. (B) UN1 mAb treatment resulted in improved survival of mice engrafted with HPB-ALL lymphoblastoid T-cells. Kaplan-Meier survival curves of HPB-ALL xenografted mice treated with control IgG$_1$ or UN1 mAb are shown. (C) UN1 mAb did not mediate complement-dependent cytotoxicity. HPB-ALL cells were pre-incubated with UN1 mAb (200 µg/ml), W6/32 mAb (100 µg/ml), IgG (200 µg/ml), or without antibodies (w/o mAb), and then incubated in presence or absence (w/o compl.) of complement for a standard complement-dependent cytotoxicity assay. The W6/32 mAb was a positive control. The mean of dead cells ± SD of each experimental point is shown. (D) UN1 mAb mediated antibody-dependent NK cytotoxicity of HPB-ALL cells. Primary cultured human NK cells derived from different donors (n=9) were allowed to bind to UN1-, W6/32-, OKT3- opsonized or not opsonized (no mAb) HPB-ALL target cells and tested in ADCC assay. The mean percentage ± SD of specific lysis at E:T ratio 6:1 is shown. The *p*-values of UN1-, W6/32-, or OKT3- specific lysis *versus* no mAb-specific lysis were calculated by paired two-tailed Student's *t* test, and are indicated by asterisks, as follows: (*) *p*=0.0026; (**) *p*=0.0008; (***) *p*=0.0001. (E) Results expressed as lytic units/10^6 cells of the ADCC assay described in D. Each curve represents a single donor.
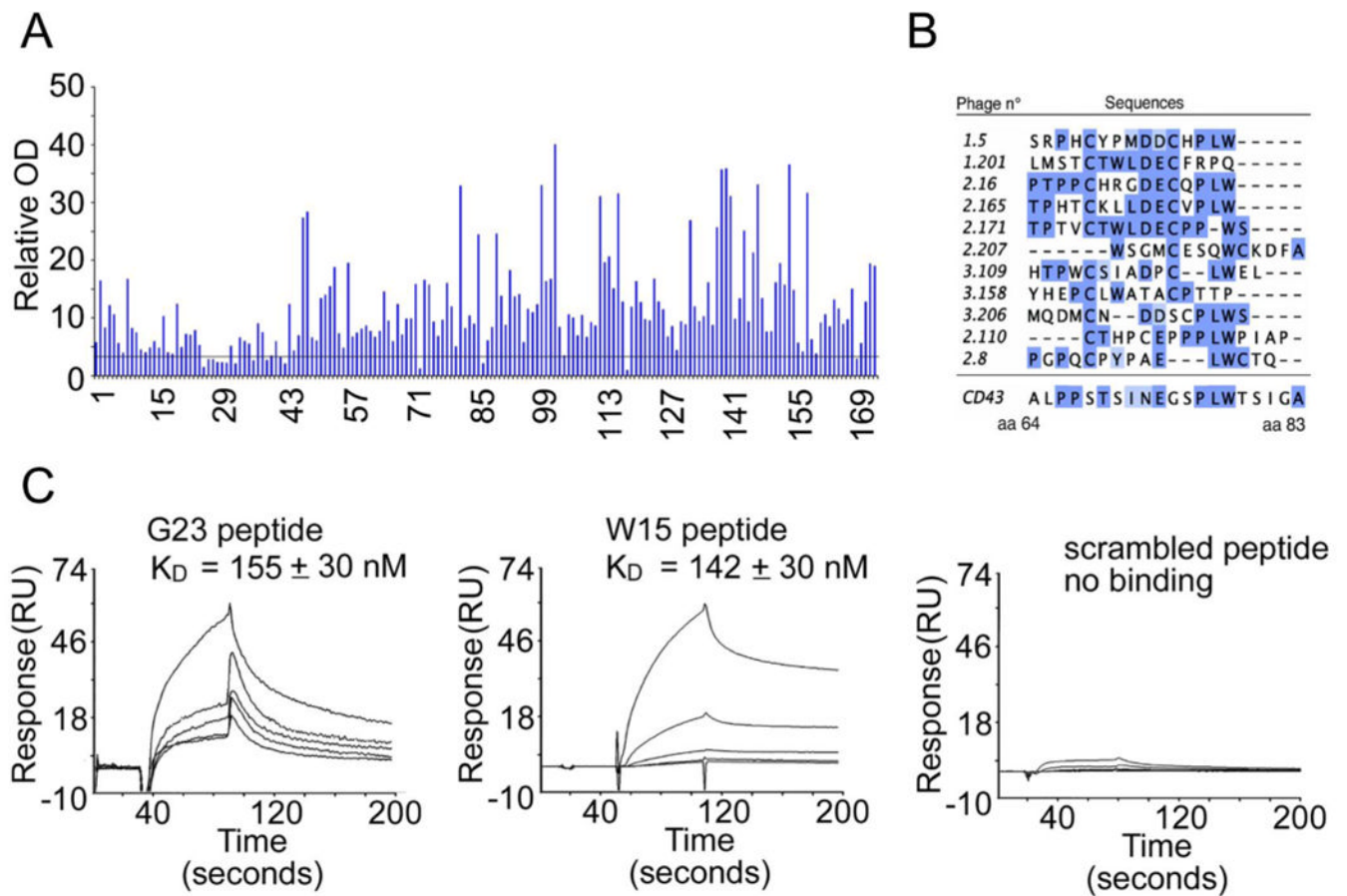
Fig. 2. Binding analysis of phagotopes and peptides to UN1 mAb

(A) ELISA binding analysis of 174 selected phages clones to UN1 mAb. Each phagotope was tested in duplicate and the relative absorbance was calculated as the difference between OD_{405nm} and OD_{620nm}. Relative OD indicates the ratio of the mean OD value of the tested phagotope to the mean OD value of the wild type phage.

(B) MUSCLE-based alignment of peptide sequence of selected phagotopes with CD43 protein. The positions of amino acids in CD43 aligned sequence are indicated.

(C) Affinity measurement of G23 and W15 peptides binding to UN1 mAb by Surface Plasmon Resonance (SPR). The sensorgrams show G23 peptide, W15 peptide and scrambled peptide binding to UN1 mAb immobilized on CM5 sensor chip. The peptide concentrations used were 0.1, 0.25, 0.5, 1.0 and 2.5 mM. The response expressed in resonance units was recorded as a function of time. For G23 and W15 peptide, the corresponding K_D is indicated.
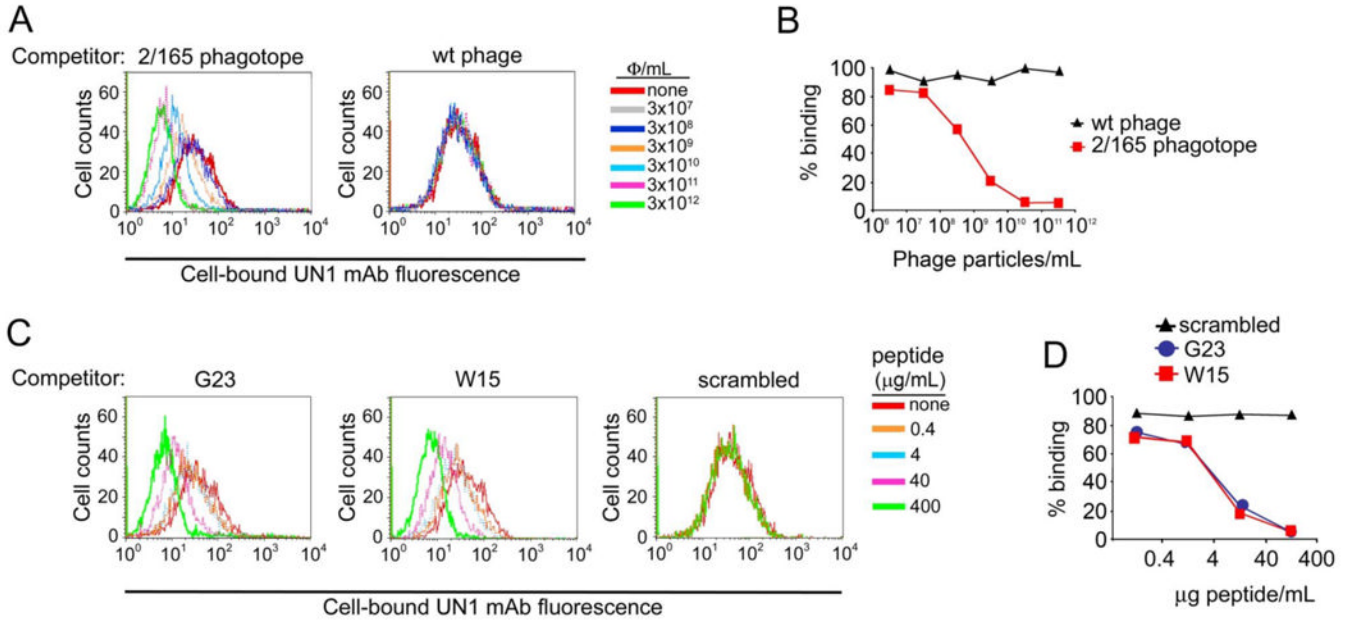
Fig. 3. Phage clone 2/165 and the derivative peptides inhibited the binding of mAb UN1 to UN1-positive cancer cells

(A) Phagotope 2/165 inhibited the UN1 mAb binding to UN1-positive HPB-ALL cells. The mAb UN1 (0.37 μg/ml) was pre-incubated with the indicated doses of 2/165 phage (left panel) or wild type phage (right panel), and then added to HPB-ALL cells (5×10^5). Cell-bound UN1 mAb was revealed by flow cytometry. Histogram overlays of the UN1 mAb fluorescence intensity are shown. (B) Percentage of HPB-ALL cells recognized by mAb UN1 for the experiment described in A. (C) Synthetic peptides G23 and W15 inhibited the UN1 mAb binding to UN1-positive HPB-ALL cells. The mAb UN1 (0.37 μg/ml) was pre-incubated with the indicated doses of G23 (left panel), W15 (middle panel) or scrambled (right panel) peptides, and then added to HPB-ALL cells (5×10^5). Cell-bound UN1 mAb was revealed by flow cytometry. Histogram overlays of the UN1 mAb fluorescence intensity are shown. (D) Percentage of HPB-ALL cells recognized by mAb UN1 for the experiment described in B.
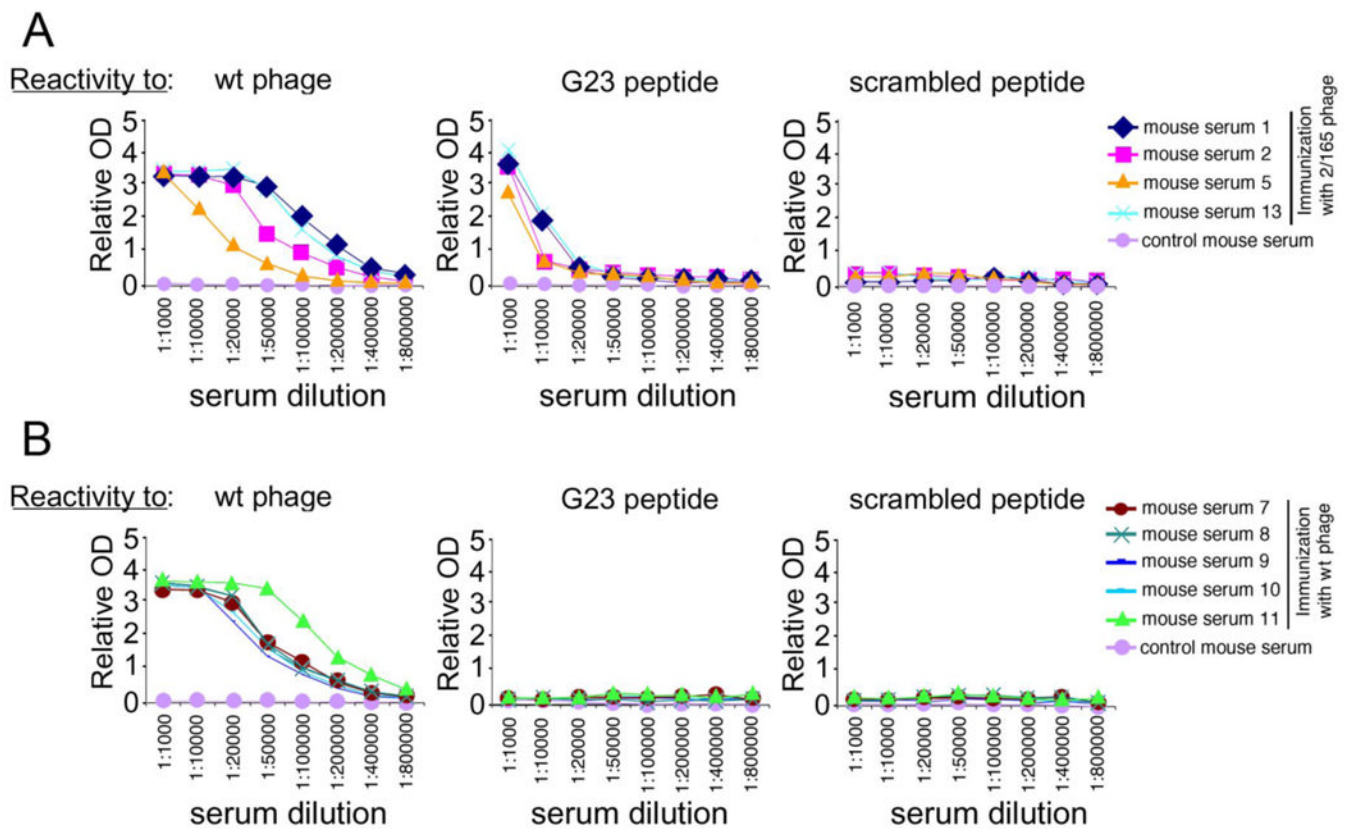
Fig. 4. Reactivity of immunized mice sera
(A,B) Reactivity against wild type phage, G23- or scrambled-peptide of sera from 2/165 phagotope-immunized mice (samples 1, 2, 5 and 13) (panel A), or wild type phage-immunized mice (samples 7, 8, 9, 10 and 11) (panel B), as evaluated by ELISA. Relative OD was calculated as the difference between OD_{405nm} and OD_{620nm}. Sera dilutions are indicated on abscissa.
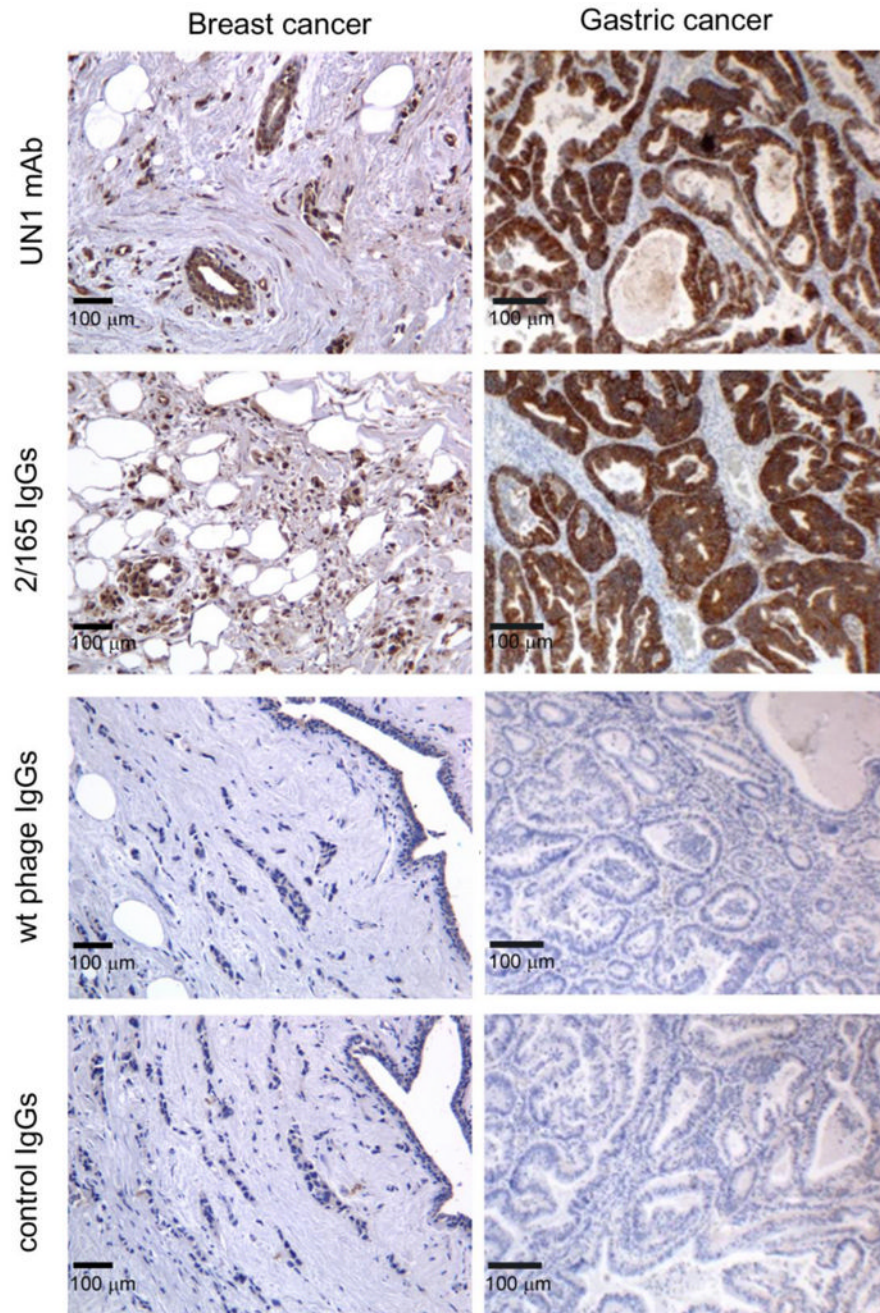
Fig. 5. The 2/165 phage-induced antibodies detected UN1-positive human breast and gastric cancer tissues
Serial sections of surgical specimens derived from breast and gastric cancer tissues were stained with UN1 mAb, 2/165 IgGs (IgGs purified from sera of 2/165 phagotope-immunized mice), wt IgGs (IgGs purified from sera of wild type phage-immunized mice) or control IgGs (IgGs purified from not-immunized mice), according to peroxidase-antiperoxidase method. Original magnification ×200.
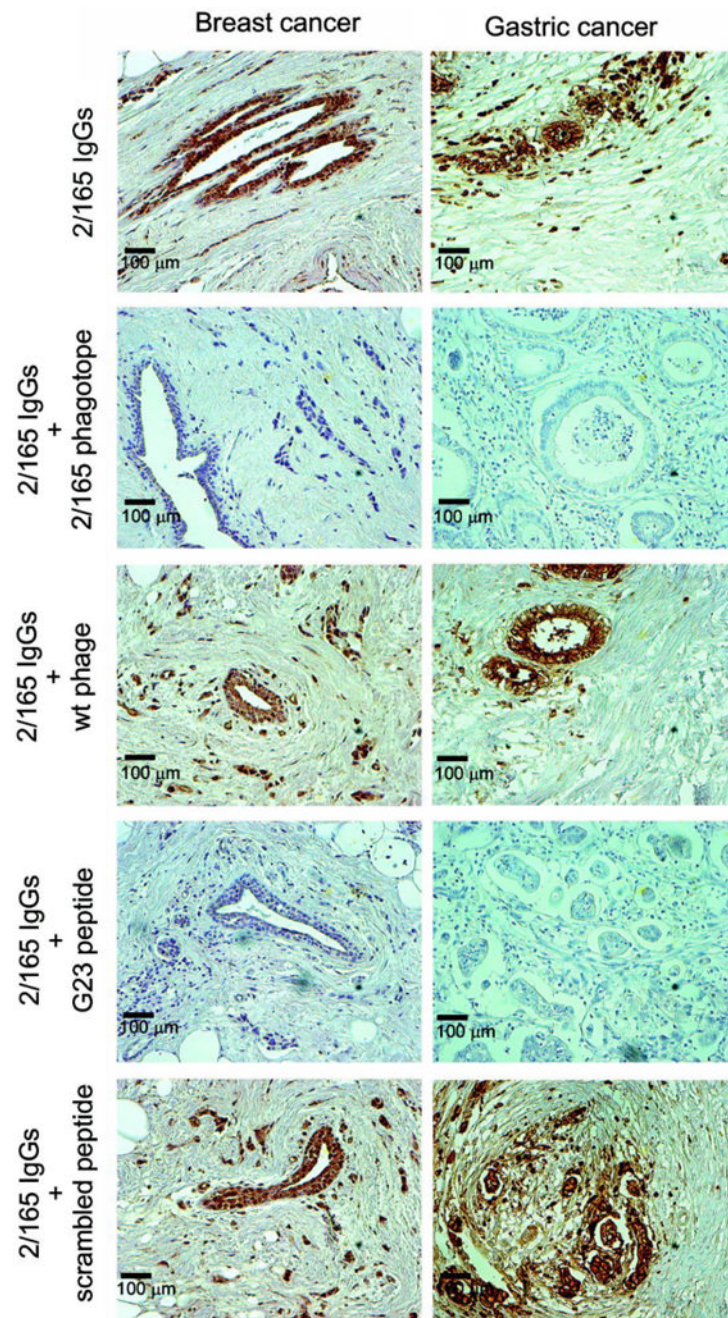
Fig. 6. The 2/165 phagotope and G23 peptide inhibited the binding of 2/165 IgG to human breast and gastric cancer tissues

Serial sections of surgical specimens derived from breast and gastric cancer tissues were stained with 2/165 IgGs, pre-incubated overnight at 4°C with the indicated phage (2.5×10^{13} phage particles/mL) or peptide (500 µg/mL), according to peroxidase-antiperoxidase method. Original magnification ×200.

Table 1
Sequences of UN1 mAb-selected mimotopes

Amino acid sequences of selected mimotopes. Frequency indicates the recurrence of the same sequence in different phage clones. OD_{405}-OD_{620} refers to the ELISA results of phage reactivity to UN1 mAb.

Phage Number	Peptide Sequence	Frequency	OD_{405}-OD_{620}
1.5	SRPHCYPMDDCHPLW	4	1.137
1.201	LMSTCTWLDECFRPQ	6	1.025
2.16	PTPPCHRGDECQPLW	5	0.703
2.165	**TPHTCKLLDECVPLW**	**3**	**2.925**
2.171	TPTVCTWLDECPPWS	1	1.052
2.207	WSGMCESQWCKDFA	4	1.039
3.109	HTPWCSIADPCLWEL	1	1.597
3.158	YHEPCLWATACPTTP	1	0.464
3.206	MQDMCNDDSCPLWS	1	0.481
2.110	CTHPCEPPPLWPIAP	1	2.082
2.8	PGPQCPYPAELWCTQ	1	0.336

Table 2
In vivo toxicity of phage immunization

Balb/c mice (5 animals/group) were immunized with the phage 2/165, or wild type phage, or left untreated, and the collected sera at days 7-10 from the 6th boost were analysed for the indicated markers of systemic toxicity. Values represent the mean ± SEM of sample measurements.

Group	IL-1β (pg/mL)	GSH (μM)	LDH (IU/L)
Untreated	58.0 ± 0.2	10.4 ± 1.2	65.4 ± 12.3
Wt phage	59.7 ± 0.3	9.8 ± 0.8	60.0 ± 11.5
2/165 phage	58.2 ± 0.3	10.1 ± 0.9	52.9 ± 15.4